Jpn. J. Appl. Phys. Vol. 34 (1995) pp. 4579–4586
Part 1, No. 9A, September 1995

Positron Annihilations Associated with Defects in Plastically Deformed Si

Atsuo KAWASUSO*, Masashi SUEZAWA, Masayuki HASEGAWA, Sadae YAMAGUCHI and Koji SUMINO

Institute for Materials Research, Tohoku University, Sendai 980, Japan

(Received March 29, 1995; accepted for publication July 3, 1995)

Deformation-induced defects in Si have been studied using positron lifetime measurement. Two lifetime components, 285 ps and 544 ps, which were assigned to dislocation-related defects and vacancy clusters, respectively, were observed. Through annealing experiments, the dislocation-related component was found to consist of two more components: one annihilated after the annealing at around 900 °C and the other remaining even at 1100 °C. These were attributed to vacancy like parts on dislocations and to dislocations themselves, respectively. Positron trapping rate due to dislocations increased upon cooling and saturated below 80 K. It was approximately proportional to the inverse of the temperature ($\sim T^{-1}$) in the temperature range between 100 and 300 K. These features were interpreted in terms of shallow levels originating from strain fields around dislocations and the one-dimensionality of dislocations.

KEYWORDS: dislocation, deformation, positron annihilation, Si

1. Introduction

Electronic and optical properties of defects in Si induced by plastic deformation have been studied by various methods, such as electron spin resonance (ESR),[1-6] deep-level transient spectroscopy (DLTS)[7-16] and photoluminescence (PL).[17-26] It is known that many kinds of ESR, DLTS and PL active centers are introduced by plastic deformation. Since some PL peaks remain even after the high-temperature annealing by which point defects are annihilated, they are thought to be related to dislocations. Most ESR and DLTS signals disappear after annealing at rather low temperature ($\leq$800 °C). They are thought to be related to point defects and their aggregates, and not to dislocations themselves since most dislocations are stable at 800 °C.

Recently, positron annihilation spectroscopy (PAS) is extensively applied to the investigations of vacancy-type defects in semiconductors, and some intriguing features associated with defects have been reported.[27-29] A few studies have so far been reported on the defects induced by plastic deformation. Dannefaer *et al.*[30] were the first to apply PAS to the study of defects in deformed Si. Recently, Krause *et al.*[31] also showed a systematic study of deformation-induced defects in Si. They deformed Si crystals with small strains at low temperature, and investigated the annealing behaviors of positron lifetime and trapping rate in the temperature range below 850 °C. Their results show that two kinds of positron trapping centers exist in deformed Si. Those centers were attributed to large vacancy clusters and dislocation-related defects. They found that the introduction rate and annealing temperature of the vacancy clusters were similar to those of ESR signals designated Si:K3–5. They suggested that the dislocation-related defects might be some vacancy like parts on dislocations, but not the dislocations themselves, since such ESR signals decreased drastically at around 700 °C where dislocations are stable. They also found similarities in annealing temperature and introduction rate between the dislocation-related component and ESR signals designated Si:K1/K2.

Although dislocations in Si are also expected to act as positron trapping and annihilation centers, this has not yet been clarified. Point defects are known to disappear at low temperature where dislocation density does not change. To show that dislocations in Si actually act as the positron trapping and annihilation centers, annealing experiments at high temperature (>850 °C) for heavily deformed Si is indispensable. Thus, we studied the annealing behaviors of defects at high temperature in heavily deformed Si, unlike the case of Krause *et al.*[31] Since the positron trapping rate due to a defect is sensitive to its charge state, the effect of Fermi level on the positron trapping rate was also studied. Moreover, to clarify the interaction between a positron and trapping centers, the temperature dependences of positron lifetime and trapping rate were also studied.

2. Experimental

Specimens were prepared from floating-zone-grown Si crystals doped with phosphorus or boron. The specimen surfaces were damaged with carborundum powder prior to deformation to introduce a high density of dislocation generation centers. Specimens were subjected to compressive deformation along the [123] direction at 800 °C in a vaccum to various strains. After the deformation, the specimens for each measurement were cut out from the center part of deformed specimens. They were finished by etching with CP4 reagant. Dislocation density N_d was counted from scanning electron microscopy (SEM) observations of the etch pit. The Fermi level E_F of the specimen was determined from the Hall effect measurements by means of the van der Pauw method. Table I summarizes the characteristics of the specimens. Isochronal annealing was performed from 600 °C to 1100 °C with temperature steps of 50 °C and the annealing duration of 30 min in the argon ambient. Isothermal annealing was also performed at various temperatures.

The positron source was prepared by depositing

*Present address: Takasaki Radiation Chemistry Research Establishment, JAERI, Watanuki-machi 1233, Takasaki 370-12, Japan.

Table I. Characteristics of specimens.

Specimen	Dopant (cm^{-3})	ε (%)[a]	N_d (cm^{-2})[b]	E_F (eV)[c]
PH-1	P: 1.5×10^{15}	7	1.5×10^{8}	$E_c-0.25$
-2		12	1.8×10^{8}	$E_c-0.25$
-3		15	2.2×10^{8}	$E_c-0.26$
-4		20	2.4×10^{8}	$E_c-0.26$
-5		29	2.9×10^{8}	$E_c-0.27$
BW-1	B: 4.0×10^{14}	9	9.7×10^{7}	$E_v+0.22$
-2		19	1.1×10^{8}	$E_v+0.27$
-3		24	1.6×10^{8}	$E_v+0.30$
BH-1	B: 1.0×10^{16}	13	2.0×10^{8}	$E_v+0.17$

[a]Resolved shear strain.
[b]Dislocation density.
[c]Fermi level.

^{22}NaCl ($\sim4\times10^{5}$ Bq) onto a Mylar thin film with a thickness of ~5 μm. It was sandwiched by two specimens and positron lifetime measurement was carried out at room temperature using a conventional spectrometer with a time resolution of $\sim$200 ps. The temperature dependence of positron lifetime was also measured in the temperature range between 10 and 300 K. The total count of $\sim2\times10^{6}$ was accumulated in each spectrum. The source component was determined to be $\sim$350 ps with the intensity of $\sim$10% from the measurement of undeformed Si. After subtracting the source and background components, lifetime spectra were resolved into two or three lifetime components using the fitting program of PATFIT-88.[32] For example, in the case of three-component analysis, a spectrum was fitted by

$$L(t)=(I_1/\tau_1)\exp(-t/\tau_1)+(I_2/\tau_2)\exp(-t/\tau_2)+(I_3/\tau_3)\exp(-t/\tau_3). \quad (1)$$

Here, τ_i ($i=1, 2, 3$) are the positron lifetimes and I_i are the intensities ($I_1+I_2+I_3=1$). The mean positron lifetime is given as

$$\tau_M=I_1\tau_1+I_2\tau_2+I_e\tau_3. \quad (2)$$

This quantity is sensitive to the increase of positron lifetime. Thus, we first check the increase of positron lifetime with this quantity. If the trapping model[33] is a good approximation, the lifetimes obtained from eq. (1) should be

$$\tau_1=\frac{1}{1/\tau_B+\kappa_{D1}+\kappa_{D2}}, \quad (3)$$

$$\tau_2=\tau_{D1}, \quad (4)$$

$$\tau_3=\tau_{D2}, \quad (5)$$

where τ_B is the positron lifetime in the bulk (220 ± 2 ps from the measurement of undeformed Si), and τ_{D1} and τ_{D2} are the positron lifetimes at different defects denoted by $D1$ and $D2$. κ_{D1} and κ_{D2} are the net trapping rates due to the defects $D1$ and $D2$, respectively:

$$\kappa_{D1}=\frac{I_2}{I_1}\{1/\tau_B-(1-I_3)/\tau_{D1}-I_3/\tau_{D2}\}, \quad (6)$$

$$\kappa_{D2}=\frac{I_3}{I_1}\{1/\tau_B-I_2/\tau_{D1}-(1-I_2)/\tau_{D2}\}. \quad (7)$$

The right-hand side of eq. (3) is independent of τ_1, hence the validity of the trapping model can be checked from the difference between τ_1 and the right hand side of eq. (3). In the two-component analysis, we neglect τ_3, I_3 and κ_{D2} in the above equations.

The trapping rate is given by

$$\kappa=\mu\cdot C=\nu_+\cdot\sigma\cdot C, \quad (8)$$

where C is the defect concentration, μ the specific trapping rate, ν_+ the thermal velocity of a positron ($\sim10^{7}(T/300)^{1/2}$ cm/s, T the temperature) and σ the trapping cross section. Thus, we can determine the values of specific trapping rate and cross section if the defect concentration is known.

3. Results

3.1 *As-deformed state*

Figure 1 shows the mean lifetimes as a function of the resolved shear strain. It is found that the mean lifetimes for each specimen increase with strain. This suggests that some open-volume-type defects are introduced by the deformation. The increase of mean lifetime of the PH specimens is the largest and that of the BH specimens is the smallest. Thus, the increase in the mean lifetime depends on the conduction type of the specimen.

In order to obtain more detailed information, lifetime spectra were decomposed into several lifetime components. Since two kinds of positron trapping centers are reported to be introduced after deformation,[30,31] lifetime spectra were decomposed into three lifetime components which correspond to bulk, center 1 and center 2. Figure 2 shows τ_1, τ_2 and τ_3, and I_2 and I_3 as a function of resolved shear strain. τ_1 agrees with that expected from the trapping model. This assures the validity of the analysis based on the trapping model. Two lifetime components $\sim$285 ps and $\sim$544 ps are introduced after the deformation in the PH specimens. This result is similar to that reported in the previous works.[30,31] The lifetimes τ_2 and τ_3 are nearly independent of strain, while their intensities increase with strain. This suggests that the species of defects acting as positron trapping centers do not change with strain, but their

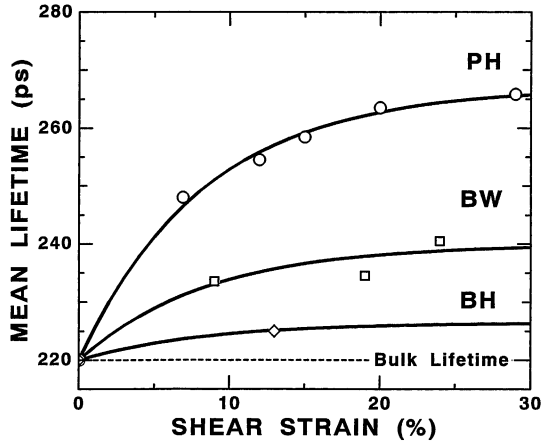

Fig. 1. Mean positron lifetimes of as-deformed states as a function of the resolved shear strain.

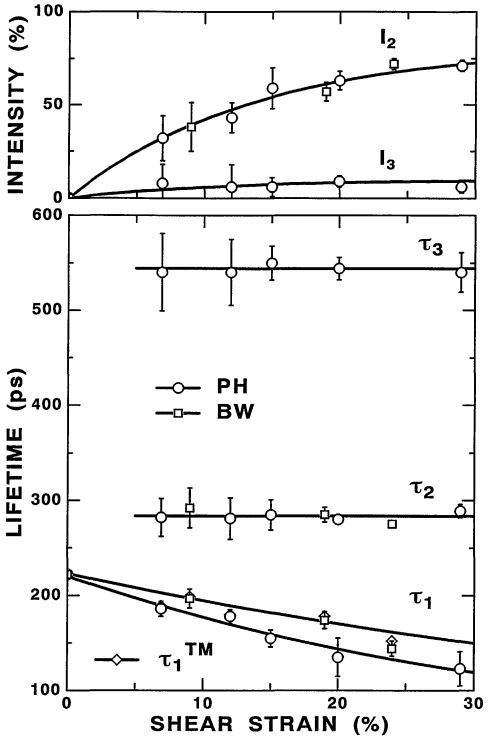

Fig. 2. The positron lifetimes τ_1, τ_2 and τ_3 and the intensities I_2 and I_3 as a function of the resolved shear strain. τ_1^{TM} denotes the lifetime τ_1 expected from the trapping model.

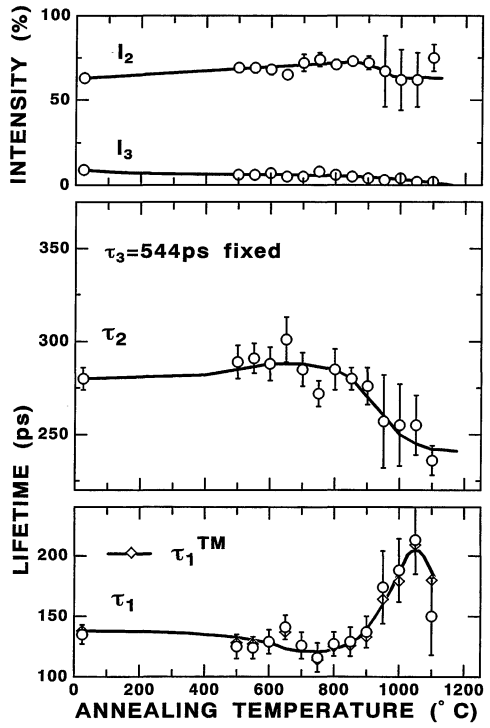

Fig. 3. The positron lifetimes τ_1 and τ_2, and the intensities I_2 and I_3 as a function of annealing temperature for the PH-4 specimens. The lifetime τ_3 is fixed to 544 ps in the analysis. τ_1^{TM} denotes the lifetime τ_1 expected from the trapping model.

concentrations increase. The lifetime of ~285 ps is also found for the BW specimens, but the lifetime of ~544 ps is not. For the BH specimen, neither the second nor third lifetime component is found, despite the fact that mean lifetime is prolonged as compared to the bulk lifetime, as shown in Fig. 1. This indicates that the lifetime at the effective trapping centers in the BH specimen is close to the bulk lifetime. Now, it is clear that the dependence of the mean lifetime on the conduction type of specimens shown in Fig. 1 is a result of the difference in the number of lifetime components according to the conduction type of specimens.

The lifetime spectrum could be decomposed into two or three components for the BW or PH specimens. However, several defect species may contribute to those components. To discriminate such species and also to show thermal stabilities of the lifetime components, annealing experiments were carried out.

3.2 *Annealing behavior*

We first present the results of isochronal annealing to show the annealing temperature of positron trapping centers. Figure 3 shows the lifetimes τ_1 and τ_2, and intensities I_2 and I_3 for the PH-4 specimen as a function of annealing temperature. Since the lifetime τ_3 was rather scattered between 500 and 600 ps due to the low signal intensity of I_3 in ordinary analysis, it was fixed to be 544 ps to minimize the statistical error in the analysis. The lifetime τ_1 agrees with that expected from the trapping model. This assures the validity of the trapping model. The dependence of lifetime τ_2 on the annealing temperature is discussed later with that of trapping

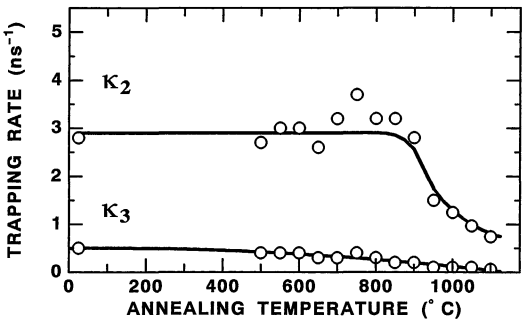

Fig. 4. The positron trapping rates as a function of annealing temperature for the second and third lifetime components shown in Fig. 3.

rate κ_2. Figure 4 shows the annealing behaviors of the trapping rates κ_2 and κ_3 responsible for the second and third lifetime components, respectively, which are calculated from the lifetimes and intensities shown in Fig. 3 using eqs. (6) and (7).

The trapping rate κ_3 decreases gradually from 800°C and becomes very small above 1000°C. The lifetime τ_2 decreases from ~285 ps to ~240 ps at around 900°C. The trapping rate κ_2 decreases with the decrease in the lifetime τ_2 but remains even after annealing at 1100°C. This result suggests that the second lifetime component consists of two more lifetime components: one disappears at around 950°C and the other remains even after 1100°C. The lifetime at the latter center is ~240 ps. That of the former is roughly estimated to be ~300 ps from the changes of lifetime τ_2 and trapping

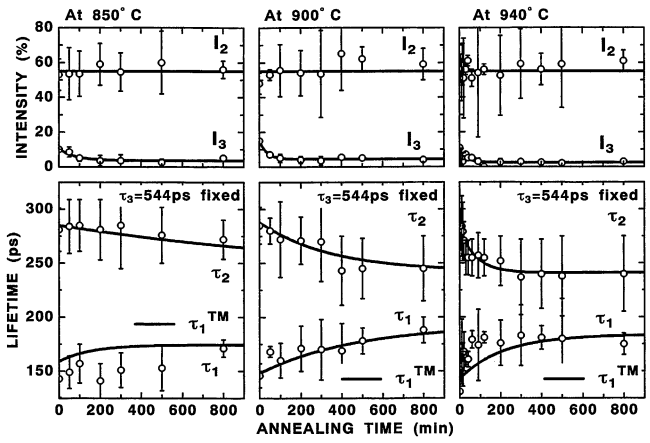

Fig. 5. The positron lifetimes τ_1 and τ_2, and the intensities I_2 and I_3 as a function of annealing time at 850, 900 and 940°C for the PH-4 specimens. τ_1^{TM} denotes the lifetime τ_1 expected from the trapping model.

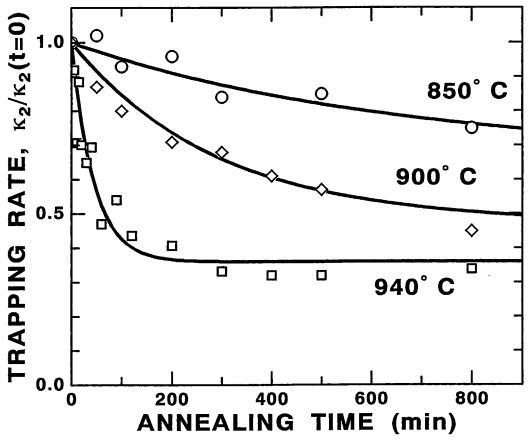

Fig. 6. The positron trapping rate as a function of annealing time for the second lifetime component shown in Fig. 5. The values of trapping rates are normalized with those of as-deformed state.

rate τ_2. Krause *et al.*[31] also observed the lifetime of ~300 ps. They reported that the component decreased drastically after the annealing at around 700°C, but remained after the annealing at 850°C. Thus, the lifetime ~300 ps observed in the present work seems to correspond to the component observed after the annealing at 850°C in Krause *et al.*'s work. The lifetime component ~240 ps which has a high thermal stability has not been reported so far.

To elucidate more detailed annealing characteristics associated with the second lifetime component (τ_2), isothermal annealings were also carried out. Figure 5 shows the lifetimes τ_1 and τ_2 and intensities I_2 and I_3 for the PH-4 specimen as a function of annealing time at 850, 900 and 940°C, respectively. The lifetime τ_3 was again fixed to 544 ps for the same reason as above. The lifetime τ_1 agrees with that expected from the trapping model. Figure 6 shows the annealing behavior of trapping rate κ_2 estimated from the lifetimes and intensities shown in Fig. 5 using eqs. (6) and (7).

The lifetime τ_2 decreases toward ~240 ps with annealing time. The trapping rate also decreases with the

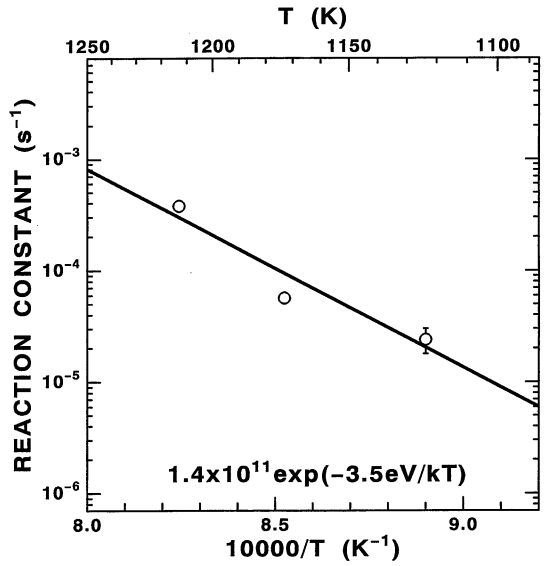

Fig. 7. The Arrhenius plot of reaction constant for the annealing of the second lifetime component shown in Fig. 6.

annealing time and has a tendency to become constant. The decrease of the lifetime τ_2 and trapping rate κ_2 at 850°C is very slow, while at 940°C it is fast. These behaviors are consistent with those of isochronal annealing shown above. Namely, the lifetime component (τ_2) consists of two more components: one (~300 ps) disappears at around 900°C and the other (~240 ps) remains after the annealing at around 900°C.

If the decrease of the trapping rate shown in Fig. 6 can be approximated by the first-order process, the annealing behavior may be written as

$$\kappa_2(t)=\kappa_{dis}\exp(-Kt)+\kappa_{res}. \quad (9)$$

Here, κ_{dis} and κ_{res} represent the disappearing and residual components, respectively. K denotes the reaction constant which is defined as $K_0\exp(-E/k_BT)\,s^{-1}$, where E is the activation energy for the process. The solid lines in Fig. 6 shows the fittings of eq. (9) to the experimental data. It is found that the results are reproduced well by eq. (9). Figure 7 shows the Arrhenius plot of the reaction constant K. The activation energy was estimated to be 3.5 ± 1.0 eV from the Arrhenius plot. We will discuss this value in §4.

3.3 *Temperature dependence*

To clarify the interaction between a positron and trapping centers, we measured the temperature dependences of positron lifetime and trapping rate below 300 K. Here, we focused on the trapping centers which remain after the annealing at 900°C. Figure 8 shows the temperature dependences of lifetimes τ_1 and τ_2, and intensities I_2 and I_3 for the PH-4 specimen which was annealed at 900°C for 800 min prior to the measurement. The lifetime τ_1 agrees with that expected from the trapping model. The lifetime τ_2 is found to be nearly constant between 10 and 300 K. The intensity I_2 increases with decreasing temperature. Figure 9 shows the temperature dependence of the trapping rate κ_2 responsible for the second component. The trapping

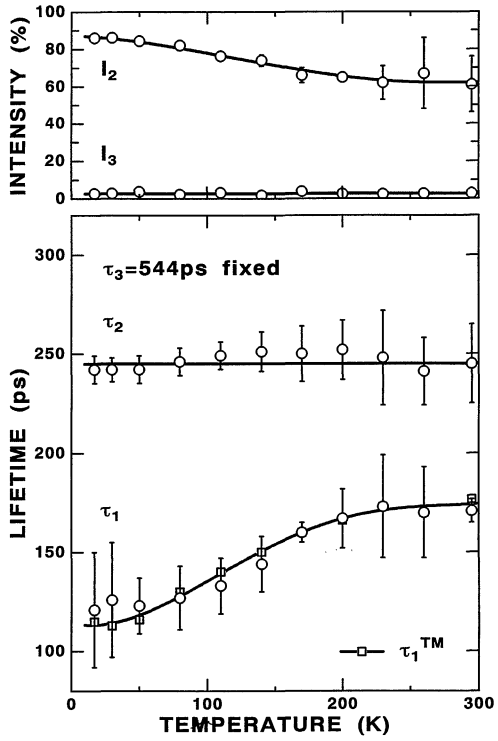

Fig. 8. The temperature dependences of the lifetimes τ_1 and τ_2, and intensities I_2 and I_3 for the PH-4 specimens after the annealing at 900°C for 800 min. τ_1^{TM} is that expected from the trapping model.

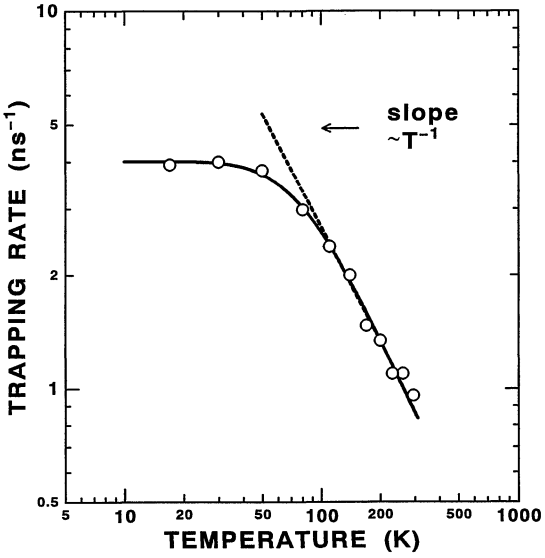

Fig. 9. The temperature dependence of positron trapping rate for the second lifetime component shown in Fig. 8.

rate is found to increase upon cooling and tend to saturate below ~80 K. It is approximated to be proportinal to T^{-1} in the temperature range between 100 and 300 K.

4. Discussion

As shown above, two lifetime components, τ_2~285 ps and τ_3~544 ps, are observed in the as-deformed specimen.

4.1 *Shorter lifetime component*

As shown in §3.2, the shorter lifetime component τ_2~285 ps observed after the deformation is a weighted average between different centers with τ_{2A}~300 ps and τ_{2B}~240 ps, respectively.

$$\tau_2 \sim 285 \text{ ps} \left\{ \begin{array}{l} \tau_{2A} \sim 285 \text{ ps} \\ \tau_{2B} \sim 240 \text{ ps} \end{array} \right.$$

The former center disappears after the annealing at around 900°C, while the latter center remains even after the annealing at 1100°C. These two centers are open-volume-type defects since they result in prolonged lifetimes. These centers may not be related to other types of defects, such as metallic impurity agglomerations due to contamination during heat treatment, since such defects do not result in prolonged lifetimes. This is confirmed from the agreement of lifetime τ_1, with that expected from the trapping model.

The lifetime τ_{2A}~300 ps indicates that the size of the open volume associated with the trapping center is comparable to that of a divacancy in Si. However, an isolated divacancy rarely survives at 800°C where deformation has taken place. This leads us to assume that this center is related to some vacancy like parts on the dislocations, as suggested by Krause *et al.*[31] Some theoretical researchers[34–39] propose that antiphase defects called solitons exist on reconstructed dislocation cores and that they play an important role in dislocation motion. Furthermore, Heggie and Jones[36–39] proposed soliton-vacancy complexes as the electrically active centers on the dislocation cores. The solitons and soliton-vacancy complexes may act as the effective trapping centers for a positron due to their open volumes. Dislocations in the crystals of the diamond structure dissociate into two partial dislocation. For instance, a screw and a 60° perfect dislocations dissociate into two 30° partial dislocations and 30° and 90° partial dislocations, respectively. Solitons or soliton-vacancy complexes can exist on these types of dislocations. From a geometrical viewpoint, the open volumes of soliton-vacancy complexes on dislocations seem to be similar to those of small vacancies, such as a monovacancy or a divacancy. Thus, such defects are expected to act as the positron trapping centers giving rise to the lifetime τ_{2A}~300 ps.

Weber and Alexander[2] reported that the anisotropy of g-tensors and hyperfine interaction tensors for the ESR signals labelled Si:K1/K2 was explained well if the centers were associated with the soliton-vacancy complex on the 30° dislocation. Krause *et al.*[31] suggested that the positron trapping center which decreased at around 700°C was likely to be responsible for Si:K1/K2 centers. Dannefaer *et al.*[30] found that the activation energy of such a component was 1.4–2.0 eV. Its magnitude is approximately equal to that for the Si:K1/K2 centers determined by Wöhler *et al.*[1] However, as mentioned in §3.2, the lifetime component τ_{2A}~300 ps observed in this work decreased at around 900°C, and its activation energy of ~3.5 eV was much higher than that for the Si:K1/K2 centers. Furthermore, it is also

higher than that determined by Kamiyama and Sumino[16] for the annihilation of defects responsible for some DLTS signals. Thus, the positron trapping center observed in this work is not related to such ESR and DLTS centers. The absence of an annealing stage at around 700°C in this work is due to a high deformation temperature (800°C) and slow cooling of the specimen after the deformation. Namely, the defects which are annealed out at around 700°C disappeared during the deformation.

Dannefaer *et al.*[30] also found a comparable activation energy for the decrease of the dislocation-related trapping rate between 915°C and 970°C. They pointed out that the value of activation energy of ~3.5 eV was close to that for self-diffusion of the Si crystal. They inferred that the presence of dislocations might alter the mechanism of self-diffusion in Si. In such a situation, thermally produced point defects at irregular parts of dislocations may diffuse and annihilate at the vacancy like parts on dislocations. An alternative explanation for the activation energy of ~3.5 eV is that it is related to the motion of the vacancy like parts on dislocations. A transmission electron microscopy (TEM) study[40] showed that dislocation dipoles, faulted dipoles, stacking faults and undefined dot like defects were eliminated, and curved dislocations were straightened after the annealing at around 900°C. This suggests that the vacancy like parts on dislocations are strictly bound at such defects, jogs or kinks, and are annihilated with them. However, this is not apparent since the activation energy of ~3.5 eV is higher than that for the glide motion of a dislocation in Si 2.2–2.5 eV.[41]

The lifetime component τ_2~285 ps is observed for the PH and BW specimens as a weighted average between two lifetime components, τ_{2A}~300 ps and τ_{2B}~240 ps. Although the mean lifetime for the BH specimen was prolonged, such a lifetime component was not resolved. The positron lifetime at the effective trapping center in the BH specimen is probably close to the bulk lifetime (*e.g.*, 230–240 ps), as seen for the other two types of specimens. The defect responsible for the lifetime τ_{2A}~300 ps may act as an effective trapping center in the PH and BW specimens, but not in the BH specimen. Considering the fact that the Fermi level depends on the conduction type of specimens as shown in Table I above result may be explained as the effect of the charge states of defects. If the defects responsible for the lifetime τ_{2A}~300 ps have a donor level between E_v+0.17 eV (Fermi level of the BH-1 specimen) and E_v+0.22 eV (Fermi level of the BW-1 specimen), the charge state changes from neutral, which can trap a positron, to positive, which cannot trap a positron, or vice versa, depending on the Fermi level position.[42] According to the theoretical study by Heggie and Jones,[37] the donor levels associated with the single dangling bond of soliton-vacancy complexes on the 30° and the 90° partial dislocations are expected to appear in the lower half of the band gap. Hence, two different charge states, neutral and positive, exist depending on the Fermi level. This also supports the above argument that the trapping center responsible for the lifetime τ_{2A}~300 ps is the soliton-vacancy complex on the dislocations.

Previous ESR and DLTS studies showed that the point defects introduced by the deformation completely disappeared due to annealing up to 900°C. As mentioned above, TEM study[40] also showed that dot like defects and faulted dipoles disappeared and curved dislocations became straight after the annealing at around 900°C. The lifetime component τ_{2B}~240 ps shows a considerably high thermal stability as compared to such point defects or irregular parts on dislocations. This leads us to conclude that the lifetime of τ_{2B}~240 ps is related to the positron annihilation at dislocations themselves. The lifetime 240 ps is intermediate between those at a monovacancy and of the bulk. Positrons annihilate at the open region associated with dislocation cores. A dislocation core may have an open cylinder along it. From a geometrical view point, the radius of such open cylinder for the core of 90° partial dislocation seems to be similar to that of a monovacancy. On the other hand, the open volume associated with the core of 30° partial dislocation may be similar to that of bulk. Thus, it seems to be reasonable to think that the lifetime of ~240 ps is a weighted average from among different types of dislocations.

As shown in §3.3, the lifetime τ_{2B}~240 ps is nearly independent of temperature between 10 and 300 K. This shows that the open volume of the dislocation core is nearly independent of temperature. The size of the open volume of the dislocation core is determined at a point of energy balance between the energy gain due to the reconstructions of dangling bonds along the dislocation core and the increase in the elastic strain energy due to the lattice distortion induced by reconstruction. Since the thermal expansion of Si crystal itself is not so large as to change the positron lifetime, the temperature dependence of elastic strain energy is expected to be small. If the reconstructed dangling bond has a bonding character, the energy gain upon reconstruction may not have strong temperature dependence due to the strong bond. On the other hand, if the reconstructed dangling bond has an antibonding character, the lattice around it may be softened due to an additional electron-lattice interaction, and hence the energy gain upon reconstruction may depend on temperature. The reconstructed dangling bonds along dislocations probably have the bonding character, and hence the thermal expansion of the dislocation core is not so large as to change the positron lifetime.

The trapping rate due to the dislocation increases with decreasing temperature and saturates below 80 K, as seen in Fig. 9. If we simply assume that a dislocation is an array of point defects, as treated by Coterill *et al.*,[43] the effective trapping radius is estimated to be ~5 Å and ~20 Å at room temperature and 15 K, respectively. The trapping radius at low temperature is much larger than the spatial extent of the dislocation core expected geometrically. Krause *et al.*[31] attempted to describe the temperature dependence of trapping rate due to dislocations in terms of the diffusion-limited regime, which required that the trapping rate be propor-

tional to the diffusion coefficient of a positron.[44] However, it seems that the diffusion limited regime does not reproduce the T^{-1}-dependence of the trapping rate and the plateau below 80 K, since the diffusion coefficient of a positron is proportional to $T^{-1/2}$ in the temperature range below 300 K.[45] It should be noted that the temperature dependence of trapping rate shown in Fig. 9 is a typical example for the trapping center which has a shallow trapping level.[46] A positron is probably first trapped by the shallow level around a dislocation and subsequently transferred to the relatively deep state in the dislocation core. A thermodynamic approach for such two-step trapping[46] gives the net trapping rate as

$$\kappa=\frac{\kappa_0\eta}{\eta+\delta}, \tag{10}$$

where κ_0 is the trapping rate by the shallow level, δ is the detrapping rate from the shallow level and η is the transition rate from the shallow level to the deep state. Manninen and Nieminen[47] gave the ratio of the detrapping and trapping rate for a dislocation as

$$\frac{\delta}{\kappa_0}=\frac{1}{N_d}\frac{m^*k_BT}{2h^2}\frac{\exp\left(-\frac{E_b}{k_BT}\right)}{\mathrm{erf}\left(\sqrt{\frac{E_b}{k_BT}}\right)}, \tag{11}$$

where m^* is the effective mass of a positron, which is almost equal to the static mass in the case of Si,[44] E_b is the energy of the shallow level, and N_d is the dislocation density. The pre-exponential factor is relate δ to the density of states for trapped and free positrons. We examined the fit of eq. (10) with eq. (11) to the experimental results using fitting parameters κ_0, E_b and η. The solid line in Fig. 9 shows the results of the fitting. The experimental result seems to be well reproduced by the two-step trapping model. The energy of the shallow level E_b was estimated to be $\sim$11 meV from the fitting. Such a shallow level may originate from the dilatational strain field around a dislocation, called the effect of deformation potential. Several theoretical works[48–52] show that the weakly bound states for an electron or a hole appear due to the deformation potential. The idea of the deformation potential was used to explain the energy positions of PL peaks related to various kinds of dislocations.[25] A long-range attraction due to the strain field probably also acts between a positron and a dislocation, and the shallow trapping levels are induced. The detrapping rated was about four times larger than the transition rate η at 300 K, but it decreased upon cooling and became negligible at 15 K. The transition rate η was estimated to be 4×10^{13} s^{-1}. It may be determined by the manner of energy dissipation, such as electron excitation and multiphonon emission. For electron excitation, the value of η is sensitive not only to the probability of electron excitation but also to the overlap integral between a positron wave function and a trapping potential. The order of magnitude varies from 10^{10} to 10^{13} s^{-1} depending on the magnitude of the overlap.[53] On the other hand, for the multiphonon emission process, η is determined as the attempt frequency of a positron from a delocalized state to a localized state. The order of magnitude is 10^{13} s^{-1} which is related to atomic vibration.[54] Although the experimentally determined value of η agrees with those for above two processes, it is not clear at present which of these processes acctually occurs.

The T^{-1}-dependence of the trapping rate between 100 and 300 K shown in Fig. 9 arises from the fact that the pre-exponential factor of eq. (11) is approximately proportional to T in that temperature range. It is interesting to note that the trapping rate of negatively charged vacancies which have the shallow trapping levels due to the Coulomb attraction are proportional to $\sim T^{-3/2}$ in the temperature range between 100 and 300 K.[55] Such a temperature dependence is explained as follows: the pre-exponential factor of δ/κ_0, which is related to the density of states of a positron, is proportional to $T^{3/2}$ as $N_V^{-1}(m^*k_BT/2\pi h^2)^{3/2}$ where N_V is the concentration of the vacancy. Thus, the different temperature dependence of the trapping rate between a dislocation (line defect) and a small vacancy (point defect) result from the difference in the density of states depending on the geometrical dimensions of the defects.

4.2 *Longer lifetime component*

It is obvious that the lifetime component $\tau_3\sim544$ ps is related to large vacancy clusters. The excess vacancies are expected to be generated due to the nonconservative motion of jogs on dislocations. It is known that the most important process in generating vacancies is the nonconservative motion of jogs on screw dislocations. Screw dislocations are expected to be introduced primarily during deformation. The jogs are mainly produced by the cuttings between different screw dislocations on the different slip planes. Vacancies produced at a spatialy localized jog probably grow easily into a large vacancy cluster. The signal intensity for the lifetime $\tau_3\sim544$ ps is rather weak, *e.g.*, $\sim$10% at most. It is probably due to the deformation mode; the specimens were deformed by "single-slip deformation" in this work where the cutting probability among dislocations was lower as compared to the case of multislip deformation.

In the early work by Dannefaer *et al.*,[30] the long lifetime component (>500 ps) observed after deformation was attributed to hexavacancies. On the other hand, Krause *et al.*[31] discussed that a hexavacancy might not give such a long lifetime due to a small decrease of the electron density in a planar arrangement of vacancies. They concluded that the vacancy clusters introduced by deformation were at least larger than a ten-vacancy cluster. A theoretical calculation by Puska and Corbel[56] and an annealing experiment by Kawasuso *et al.*[57] actually show that the lifetime at a hexavacancy is $\sim$400 ps, which is much shorter than 544 ps. These also support the suggestion of Krause *et al.*[31] However, it is difficult to determine the exact size of the vacancy cluster from the present theory with the local density approximation, since it could not produce a lifetime exceeding 500 ps. To determine the size of vacancy clusters more precisely, it is necessary to ob-

serve them by high-resolution transmission electron microscopy.

The lifetime $\tau_3 \sim 544$ ps was observed for the PH specimens, but not for the BW or BH specimens. Considering the fact that the Fermi levels for these specimens are different, as seen in Table I, this feature can be explained in terms of the charge state of the defect. The defect responsible for the lifetime of ~ 544 ps probably has an energy level between $E_v + 0.30$ eV (Fermi level of the BW-3 specimen) and $E_c - 0.26$ eV (Fermi level of the PH-3 specimen) and hence, two different charge states depending on the position of the Fermi level. As a result, the positron trapping rate may change with the Fermi level.

5. Conclusions

The deformation-induced defects were investigated by means of positron lifetime measurement. Two kinds of lifetime components were observed after the deformation. One is related to large vacancy clusters developed during the deformation. The other is related to the dislocations. Through the annealing experiments, the dislocation-related component was found to consist of two morecomponents: one is the vacancy like parts on the dislocation cores and the other is dislocations themselves. The former defects probably have a donor level in the lower half of the band gap. They were annealed at around 900°C with an activation energy of ~ 3.5 eV. The positron trapping rate by dislocations was found to increase upon cooling and to saturate at a low temperature. The trapping rate showed T^{-1}-dependence in the temperature range between 100 and 300 K. These temperature characteristics of the trapping rate were interpreted in terms of shallow trapping levels due to the dilatational strain fields around dislocations and the one-dimensional character of dislocations.

Acknowledgements

We are grateful to Dr. I. Yonenaga and Dr. Y. Minonishi for their help in the deformation of specimens.

1) F. D. Wöhler, H. Alexander and W. Sander: J. Phys. Chem. Solids **31** (1970) 1381.
2) E. R. Weber and H. Alexander: J. Phys. C (Paris) **6** (1979) 101.
3) M. Suezawa, K. Sumino and M. Iwaizumi: Inst. Phys. Conf. Ser. **59** (1981) 407.
4) R. Erdmann and H. Alexander: Phys. Status Solidi A **55** (1979) 251.
5) M. Brohl, C. Kisielowski and H. Alexander: Appl. Phys. Lett. **50** (1987) 1733.
6) C. Kisielowski, J. Palm, B. Bolling and H. Alexander: Phys. Rev. B **44** (1991) 1588.
7) J. R. Patel and L. C. Kimerling: J. Phys. C (Paris) **6** (1979) 67.
8) L. C. Kimerling and J. R. Patel: Appl. Phys. Lett. **34** (1979) 73.
9) J. R. Patel and L. C. Kimerling: Cryst. Res. Tech. **16** (1981) 187.
10) W. Szkielko, O. Breitenstein and R. Pickenhein: Cryst. Res. Tech. **16** (1981) 197.
11) V. V. Kveder, Yu. A. Ossipyan, W. Schröter and G. Zoth: Phys. Status Solidi A **72** (1982) 701.
12) H. Ono and K. Sumino: J. Appl. Phys. **57** (1985) 287.
13) C. Kisielowski and E. R. Weber: Phys. Rev. B **44** (1991) 1600.
14) P. Omling, E. R. Weber, L. Montelius, H. Alexander and J. Michel: Phys. Rev. B **32** (1985) 6571.
15) E. R. Weber and H. Alexander: J. Phys. C (Paris) **4** (1983) 319.
16) H. Kamiyama and K. Sumino: *Defect Control in Semiconductors*, ed. K. Sumino (North-Holland, Amsterdam, 1989) p. 1423.
17) N. A. Drozdov, A. A. Patrin and V. D. Tkachev: JETP Lett. **23** (1976) 597.
18) N. A. Drozodv, A. A. Patrin and V. D. Tkachev: Phys. Status Solidi B **83** (1977) K137.
19) N. A. Drozdov, A. A. Patrin and V. D. Tkachev: Phys. Status Solidi A **64** (1981) K63.
20) M. Suezawa, Y. Sasaki, Y. Nishina and K. Sumino: Jpn. J. Appl. Phys. **20** (1981) L537.
21) M. Suezawa and K. Sumino: Phys. Status Solidi A **78** (1983) 639.
22) M. Suezawa, Y. Sasaki and K. Sumino: Phys. Status Solidi A **79** (1983) 173.
23) R. Sauer, J. Weber and J. Stolz: Appl. Phys. A **36** (1985) 1.
24) R. Sauer: Mater. Sci. Forum **10–12** (1986) 763.
25) Yu. Lelikov, Yu. Rebane, S. Ruvimov, D. Tarhin, A. Sitnikova and Yu. Shreter: Mater. Sci. Forum **83–87** (1992) 1321.
26) V. Higgs, E. C. Lightowlers, C. E. Norman and P. Kightley: Mater. Sci. Forum **83–87** (1992) 1309.
27) For example, S. Dannefaer: *Defect Control in Semiconductors*, ed. K. Sumino (North-Holland, Amsterdam, 1989) p. 1561.
28) For example, P. A. Kumar, K. G. Lynn and D. O. Welch: J. Appl. Phys. **76** (1994) 4935.
29) For example, M. J. Puska and R. M. Nieminen: Rev. Mod. Phys. **66** (1994) 841.
30) S. Dannefaer, N. Fruensgaard, S. Kupca, B. Hogg and D. Kerr: Can. J. Phys. **61** (1983) 451.
31) R. Krause, M. Brohl, H. S. Leipner, Th. Drost, A. Polity, U. Beyer and H. Alexander: Phys. Rev. B **47** (1993) 13266.
32) P. Kirkegaard, N. J. Pederson and M. Eldrup: PATFIT-88, Riso-M-2704 (1989).
33) *Positron Solid State Physics*, eds. W. Bandt and A. Dupasquier (North Holland, Amsterdam, 1983).
34) P. B. Hirsch: J. Phys. C (Paris) **6** (1979) 3.
35) P. B. Hirsch: J. Phys. C (Paris) **6** (1979) 117.
36) R. Jones: Inst. Phys. Conf. Ser. **60** (1981) 45.
37) M. Heggie and R. Jones: J. Phys. C (Paris) **4** (1983) 43.
38) M. Heggie and R. Jones: Philos. Mag. B **48** (1983) 365.
39) M. Heggie and R. Jones: Philos. Mag. B **48** (1983) 379.
40) I. Yonenaga and K. Sumino: Phys. Status Solidi A **137** (1993) 611.
41) M. Imai and K. Sumino: Philos. Mag. A **47** (1983) 599.
42) The Fermi level mentioned here is defined for the whole of a specimen. It is not established that the Fermi level is strictly equal to the local Fermi level around a dislocation due to the band-bending effect. Accordingly, the energy level of defect inferred here should be regarded as applicable for normal bands, but not bent bands.
43) R. M. J. Coterill, K. Petersen, G. Trumpy and J. Träff: J. Phys. F **2** (1972) 459.
44) W. Brandt: Appl. Phys. **5** (1974) 1.
45) E. Soinen, J. Mäkinen, D. Beyer and P. Hautojärvi: Phys. Rev. B **46** (1992) 13104.
46) M. J. Puska, C. Corbel and R. M. Nieminen: Phys. Rev. B **41** (1990) 9980.
47) M. Manninen and R. M. Nieminen: Appl. Phys. A **26** (1981) 93.
48) R. Landauer: Phys. Rev. **94** (1954) 1386.
49) V. Celli, A. Gold and R. Thomson: Phys. Rev. Lett. **8** (1962) 96.
50) H. Teichler: Inst. Phys. Conf. Ser. **23** (1975) 374.
51) S. Winter: Phys. Status Solidi B **79** (1977) 637.
52) S. Winter: Phys. Status Solidi B **90** (1978) 289.
53) M. J. Puska, C. Corbel and R. M. Nieminen: Phys. Rev. B **41** (1990) 9980.
54) H. Sumi: Phys. Rev. B **27** (1983) 2374.
55) For example, J. Makinen, P. Hautojarvi and C. Corbel: J. Phys. Condensed Matter **4** (1992) 5137.
56) M. J. Puska and C. Corbel: Phys. Rev. B **38** (1988) 9874.
57) A. Kawasuso, M. Hasegawa, M. Suezawa, S. Yamaguchi and K. Sumino: Mater. Sci. Forum. **175–178** (1995) 423.